

Resonances in photoabsorption spectra of SiF_4 , $\text{Si}(\text{CH}_3)_4$, and SiCl_4 near the silicon K edge

S. Bodeur

*Laboratoire pour l'Utilisation du Rayonnement Electromagnétique, Bâtiment 209 D, Université de Paris-sud,
91405 Orsay Cedex, France*
and *Laboratoire de Chimie-Physique, 11 Rue Pierre et Marie Curie, 75231 Paris Cedex 05, France*

I. Nenner

*Laboratoire pour l'Utilisation du Rayonnement Electromagnétique, Bâtiment 209 D, Université de Paris-sud,
91405 Orsay Cedex, France*
and *Département de Physico-Chimie, Commissariat à l'Energie Atomique, Centre d'Etudes Nucléaires de Saclay,
91191 Gif-sur-Yvette Cedex, France*

P. Millie

*Département de Physico-Chimie, Commissariat à l'Energie Atomique, Centre d'Etudes Nucléaires de Saclay,
91191 Gif-sur-Yvette Cedex, France*

(Received 21 March 1986)

Photoabsorption spectra of tetrachlorosilane, tetramethylsilane, and tetrafluorosilane have been measured using synchrotron radiation in the 1830–1900-eV photon-energy range, i.e., in the vicinity of the silicon $1s$ edge. Intense resonances are observed in the discrete and the continuum part of the spectrum, and compared with previously published photoabsorption spectra obtained near the silicon $2s$ and $2p$ edges. Resonances in the discrete part of the spectrum are qualitatively interpreted using structural and electronic properties of the core-equivalent PX_4 ($X = \text{F}$, CH_3 , or Cl) phosphoranyl radicals. The interpretation of features in the continuum are discussed in terms of shape resonances, within the tetrahedral geometry.

I. INTRODUCTION

Many of the resonances which are generally observed in core-level photoabsorption spectra of molecules occur equally in the gas and solid states.^{1,2} They are of particular interest because either they are quasidiscrete excited states resulting from the promotion of a core electron (thus localized on an atomic site) into a low-lying empty molecular orbital, or they are shape resonances³ resulting from the anisotropy of the molecular field experienced by the outgoing core electron. Actually, this classification is somewhat artificial because some core excited states may well be described using the shape resonance picture. Nevertheless, for the sake of clarification, we will distinguish resonances in the discrete as type I, from resonances in the continuum as type II. Both kinds of resonances differ from Rydberg states^{4,5} and multiexcited states⁶ because the latter appear often as much weaker structures⁷ and Rydberg states almost disappear for nonhydride molecules⁸ and in spectra obtained in the condensed phase.¹

These two types of resonances nicely combine atomic and molecular character because they are specific of a given atomic-core spectrum and they give an image of the electronic structure of the molecule through their energy E , intensity, and width. For each resonance one defines a term value $T_i = P_i - E$, where P_i is the ionization potential of the considered core electron i . Using a simple model for type-I resonances, as discussed recently,^{9,10} T_i is directly related to the energy ϵ_{k^*} of the empty valence orbital k^* , measured with respect to vacuum level by the

relationship $T = \epsilon_{k^*} + J(ik^*) - K(ik^*) + \mathcal{A}$, where \mathcal{A} is the difference between core relaxation and correlation effects in the ion and in the core-excited neutral molecule, and $J(ik^*)$ and $K(ik^*)$ are the usual Coulomb and exchange integrals. If one assumes in a first approximation that the $J(ik^*) - K(ik^*) + \mathcal{A}$ contribution is independent of the core hole, one can compare directly for a given molecule the relative energies of resonances, measured near different core edges.^{10–13} This transferability of term values is very useful for assigning experimentally the symmetry of the empty (or virtual) molecular orbital, because each of them can be populated from different core levels and one can use electric-dipolar-transition selection rules.

Another important property of core-excited molecular states (type-I resonances) is contained in the equivalent-core approximation^{14,15} In this model, the valence-electron cloud “feels” the core as it was replaced by the subsequent atom in the Periodic Table. Moreover, the number of valence electrons increases by one. Consequently, term values measured in a core photoabsorption spectrum of a given molecule can be compared directly with those of the equivalent core species, but measured for valence excitation. This model has been very successful analyzing resonances near core edges in diatomic^{16,17} and even triatomic molecules.^{10,18,19}

In this paper, we present what may be the first photoabsorption spectra of tetramethylsilane (TMS), $\text{Si}(\text{CH}_3)_4$, and tetrafluorosilane SiF_4 , obtained near the silicon $1s$ edge, around 1850 eV photon energy. We also present the

Si $1s$ photoabsorption spectrum of tetrachlorosilane SiCl_4 , which will be compared with the early work of Mott.²⁰

To interpret the observed resonances:

(i) We compare the present Si $1s$ (or K) spectra with other available photoabsorption spectra and electron-energy-loss-spectra (EELS) or photofragmentation spectra (mass spectrometry technique) obtained near other core edges of the central atom, i.e., Si $2s$ (Si L_1) for TMS (Ref. 21) and SiF_4 (Ref. 1), Si $2p$ (or Si $L_{II,III}$) for SiCl_4 (Ref. 22), TMS (Refs. 21, 22, and 24), and SiF_4 (Refs. 1, 25, and 26). We will be using available calculations made either for the discrete or for the continuum part of the spectrum in SiF_4 (Refs. 1, 9, 27, and 28) and SiCl_4 (Refs. 27 and 29).

(ii) We compare for each molecule the core spectra with the equivalent core species PX_4 ($X = \text{F}, \text{CH}_3, \text{Cl}$) where the phosphorus atom replaces the silicon with a core vacancy.¹⁴ Special emphasis is placed on the structural properties of such compounds, which must be taken into account¹⁸ for applying the core-equivalent model. Here, we consider the special case of multicoordinated systems, for which large differences of equilibrium geometry between the initial Si X_4 and the core excited Si X_4^* states, explain the general features of core-photoabsorption spectra.

II. EXPERIMENTAL

Photoabsorption spectra were obtained using an experimental setup described previously,^{10,30} installed at Laboratoire pour l'Utilisation du Rayonnement Electromagnétique (LURE), using synchrotron radiation from the Anneau de Collisions d'Orsay (ACO) storage ring. Briefly, a double-crystal mounting monochromator $(-1, +1)$, equipped with two InSb(111) crystals ($2d = 7.46 \text{ \AA}$) provides a photon beam with an intensity of the order of 10^5 photons/s in a 0.4-eV band pass, around 1850 eV. This monochromatic beam passes through a 143-mm cell limited by two 10-mm-diameter windows made of 1- μm -thick polypropylene, whose transmission, in the considered spectral range, is better than 90%. The thickness of the windows is sufficient to bear the pressure difference between the cell (a few torr) and the monochromator (10^{-6} torr). The detection of the transmitted x-ray beam is ensured by a flow-proportional counter filled with a 90-10 argon- CH_4 mixture at the pressure of 400 torr.

Tetramethylsilane (TMS), normally a liquid at room temperature, is commercially available from the Janssen Chemical Company with a purity of 99.9%. It was used without further purification other than repeated freeze-pump thaw cycles to remove dissolved gases. SiF_4 and SiCl_4 , gases at room temperature, are commercially available from Prodair Company with a purity of 99.5% and 99.999%, respectively. They were introduced in the cell without further purification. Typical pressures were varied between 1 and 10 torr, in order to avoid "pressure effect" and to have a good contrast between the spectral features under study and the continuum.

The transmitted spectrum through the full (I) and empty cell (I_0) were obtained by scanning automatically the photon wavelength in two successive runs. Corrections for the decay of the source radiation were introduced

in the course of data reduction. The absorption spectra are extracted simply from $\ln(I_0/I)$ and put on a relative-intensity scale. The photon-energy calibration was determined from the measured Bragg angles, corrected for zero errors and crystal dispersion. For this energy calibration we have recorded the spectrum near the silicon K edge of a solid screen of SiC:H and compared it to the spectrum obtained by Senemaud³² by means of a 25-cm bent crystal spectrograph equipped with a gypsum crystal and calibrated with the $M\beta$ emission line of tungsten. This calibration has an accuracy of ± 0.5 eV for the absolute energies.

III. RESULTS

The photoabsorption spectra of the three molecules SiCl_4 , TMS, and SiF_4 in the vicinity of the silicon $1s$ ioni-

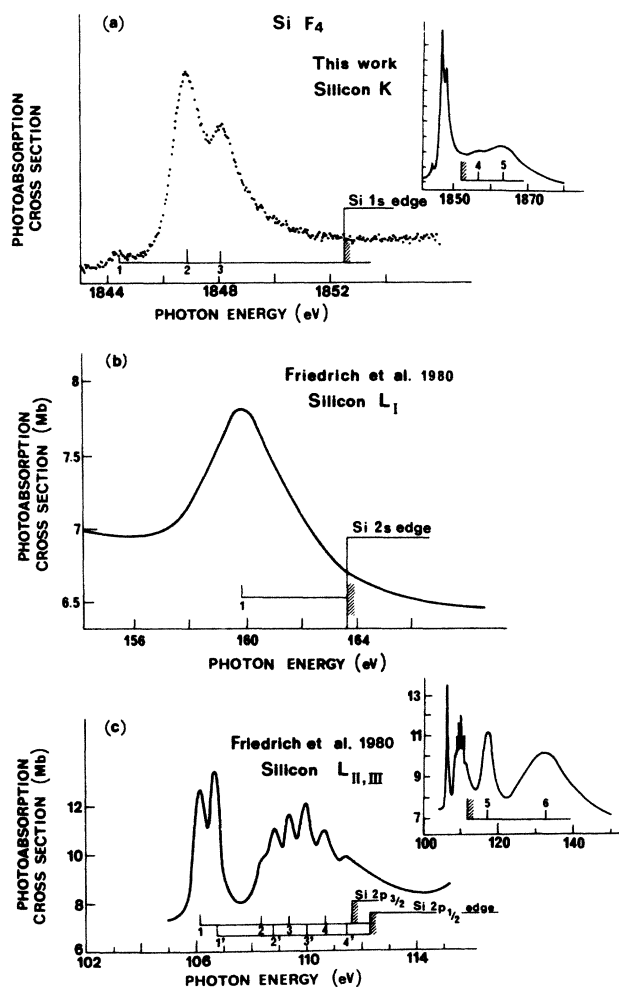


FIG. 1. (a) Silicon $1s$ (this work), (b) silicon $2s$ (Ref. 1), and (c) silicon $2p$ (Ref. 1) photoabsorption spectra of SiF_4 . The cross sections are in arbitrary units for (a) and in absolute units for (b) and (c). Full spectra are reported in insets in (a) and (c). The three edges are aligned on a vertical line and the photon energy axes have been drawn on the same relative energy scale. The resonance maxima are indicated by numbers.

zation edge region are described in detail below. This method provides the energies of the resonances on an absolute scale as seen in Sec. II. Because the understanding of the present results is also based upon knowledge of $1s$ -ionization thresholds, we also present in this section a critical analysis of experimental values of Si $1s$ edges extracted from x-ray emission or x-ray photoelectron spectra.

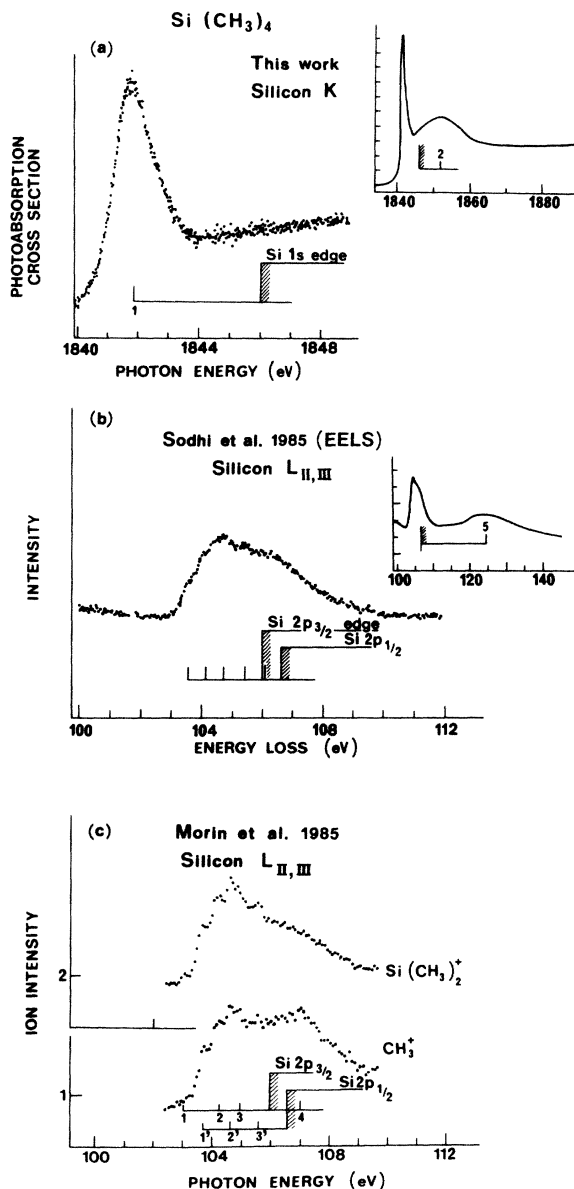


FIG. 2. (a) Silicon $1s$ (this work) photoabsorption spectrum of tetramethylsilane, (b) electron energy loss spectra (Ref. 21), and (c) selected photofragmentation spectra (Ref. 22) near the silicon $2p$ edge. The full spectra are reported in insets. The two edges are aligned on a vertical line and the photon energy axes have been drawn with the same relative scale. The resonance maxima are indicated by numbers [Figs. 2(a) and 2(c)].

A. Photoabsorption spectra

We present in Fig. 1(a) the experimental absorption spectrum of SiF₄ obtained in the 1843–1856-eV photon-energy range, at a cell pressure of 2 torr. The full spectrum (1840–1880 eV) is reported in the inset of the figure. We observe two intense resonances (labeled 2 and 3) in Fig. 1(a) in the discrete part of the spectrum, respectively located at 1846.8 and 1848.0 eV. A much weaker structure is observed at 1844.3 eV [labeled 1 in Fig. 1(a)]. In addition, a wide resonance is observed in the continuum at 1863 eV with a shoulder at 1856 eV and extending over ~ 12 eV.

We also present available photoabsorption spectra of SiF₄ obtained near the Si $2s$ [Fig. 1(b)] and the Si $2p$ [Fig. 1(c)] edges, by Friedrich *et al.*¹ The energies of these resonances (this work and Ref. 1) are reported in Table I.

We present in Fig. 2(a) the first experimental absorption spectrum of TMS obtained in the vicinity of the Si $1s$ edge, in the 1840–1849-eV photon-energy range, at a cell pressure of 5 torr. The full spectrum (1834–1888 eV) is reported in the inset of the figure. In the discrete part of the spectrum we observe a single resonance located at 1841.7 eV. This resonance is not symmetric and shows a tail on the high-energy side. The second resonance is, in contrast, observed in the continuum at 1852.1 eV and extending over ~ 12 eV.

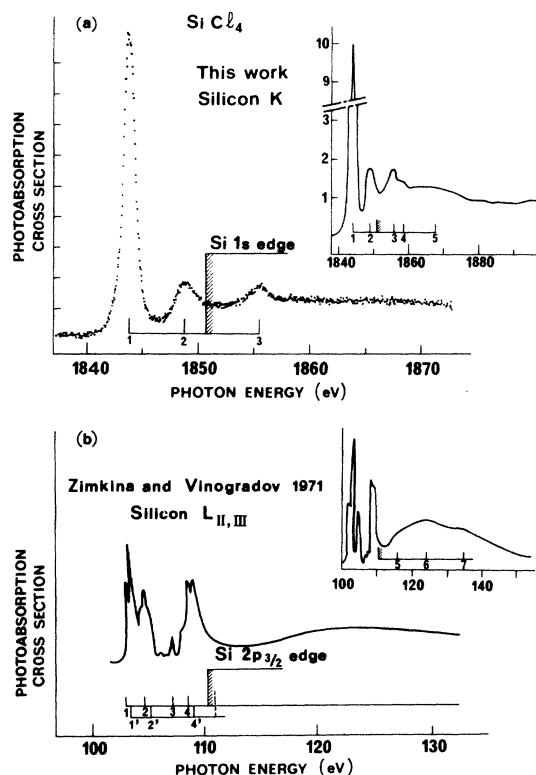


FIG. 3. (a) Silicon $1s$ (this work) and (b) silicon $2p$ (Ref. 23) photoabsorption spectra of SiCl₄. The full spectra are reported in insets. The Si $1s$ and Si $2p$ edges are aligned on a vertical line and the photon energy axes have been drawn with the same relative scale. The resonance maxima are indicated by numbers.

We also present in Fig. 2(b) the Si 2*p* EELS obtained by Sodhi *et al.*²¹ and the Si(CH₃)₂⁺ and CH₃⁺ fragment photoionization yield obtained by Morin²² using the mass spectrometry method combined with tunable synchrotron radiation in the vicinity of the Si 2*p* edge. The resonance maxima of Fig. 2(b) appear as more or less regularly spaced weak features. They have been fully confirmed by Morin²² [Fig. 2(c)] who actually saw evidence of addition-

al structure at lower energy and resolved the third feature observed by Sodhi *et al.*²¹ into two structures. The last feature reported by Sodhi *et al.*²¹ right above the 2*p*_{3/2} edge was found to be 1 eV toward higher energies by Morin and is considered to be part of the continuum. We have chosen then to renumber the six features of the discrete spectrum as reported in Fig. 2(c) and separate them into two groups associated with the $\frac{3}{2}$ and $\frac{1}{2}$ spin-

TABLE I. Absolute energies (eV), term values (eV), and proposed assignments (virtual orbital) for resonances observed in the inner-shell spectra of SiF₄.

(a) Silicon 1 <i>s</i> (photoabsorption, this work)					
Peak	Energy (eV)	Term value (eV)	Assignment ^a <i>C</i> _{2<i>v</i>} or <i>T</i> _{<i>d</i>}		
1	1844.3	8.0	<i>a</i> ₁ [*]		
2	1846.8	5.7	<i>b</i> ₁ [*] , <i>b</i> ₂ [*] , <i>a</i> ₁ [*]		
3	1848.0	4.3			
<i>P</i> ^b	1852.5	0			
4	1856	-3.7	<i>t</i> ₂ [*]		
5	1863	-10.7	<i>t</i> ₂ [*]		
(b) Silicon 2 <i>s</i> (photoabsorption, Ref. 1)					
Peak	Energy (eV)	Term value (eV)	Assignment, ^a this work <i>C</i> _{2<i>v</i>}		
1	160	3.6	unresolved (<i>b</i> ₁ [*] , <i>b</i> ₂ [*] , <i>a</i> ₁ [*])		
<i>P</i> ^b	163.6	0			
(c) Silicon 2 <i>p</i> (photoabsorption, Ref. 1)					
Peak	Energy (eV)	Term values		Assignment, ^a this work <i>C</i> _{2<i>v</i>} or <i>T</i> _{<i>d</i>}	
		$\frac{3}{2}$	$\frac{1}{2}$	$\frac{3}{2}$	$\frac{1}{2}$
1	106.13	5.47		<i>a</i> ₁ [*]	
1'	106.68		5.53		<i>a</i> ₁ [*]
2	108.4	3.2 } 3.3 }		<i>b</i> ₁ [*] , <i>b</i> ₂ [*] , <i>a</i> ₁ [*]	
2'	108.9				
3	109.4	2.2 } 2.2 }		<i>b</i> ₁ [*] , <i>b</i> ₂ [*] , <i>a</i> ₁ [*]	
3'	110.0				
4	110.7	0.9 } 0.8 }		<i>b</i> ₁ [*] , <i>b</i> ₂ [*] , <i>a</i> ₁ [*]	
4'	111.4				
$\frac{3}{2}$ <i>P</i> ^c	111.6	0			
$\frac{1}{2}$ <i>P</i> ^c	112.21	0			
5	117.2	-5.3 ^d		<i>e</i> ^{*c}	
6	133	-21.1 ^d		<i>t</i> ₂ ^{*c}	

^aThis assignment is made using the *C*_{2*v*} symmetry group for type-I resonances and *T*_{*d*} for type-II resonances.

^bSee text.

^cReference 34.

^dUsing an average value for the 2*p*_{3/2}, 2*p*_{1/2} components.

^eReference 23.

orbit components expected from the $2p$ hole. All resonance maxima are indicated by numbers and their energies are reported in Table II. Notice that the Si $2s$ EELS has been measured by Sodhi *et al.*²¹ However, the extremely small amplitude of the $2s$ resonances prevented us from reproducing the spectrum in Fig. 2. Nevertheless, this observation will be included in the discussion.

We now present in Fig. 3(a) the experimental absorption spectrum of SiCl_4 obtained in the 1837–1873-eV photon-energy range, at a cell pressure of 10 torr. The extended spectrum up to 1900 eV is shown in the inset. The general shape of this spectrum is in good agreement with the previously published data of Mott,²⁰ which, however, were presented only on a photon-energy scale relative to the first strong resonance.

We observe an intense and sharp resonance at 1843.8 eV

accompanied by a less-intense one at 1848.8 eV which belong to the discrete part of the spectrum. We also observe, in the continuum, at 1855.5, 1858.3, and 1872.6 eV, three other resonances, the high-energy one being much broader than the two low-energy ones. Notice that the 1858.3-eV resonance reported here was not observed by Mott²⁰ probably because of poorer resolution. We also present in Fig. 3(b) the photoabsorption spectrum of SiCl_4 near the Si $2p$ edge, obtained by Zimkina and Vinogradov²³ in the 100–135-eV photon-energy range.

B. Core ionization edges

In order to identify the discrete part of the present photoabsorption spectra, we have used exclusively experimental values of core ionization edges for the three molecules

TABLE II. Absolute energies (eV), term values (eV), and proposed assignments (virtual orbital) for resonances observed in the inner-shell spectra of TMS.

(a) Silicon 1s (photoabsorption, this work)										
Peak	Energies (eV)		Term value (eV)		Assignment ^a C_{2v} or T_d					
1	1841.7		4.4		unresolved b_1^*, b_2^*, a_1^*					
P^b	1846.1		0							
2	1852.1		-6.0		t_2^*					
(b) Silicon 2s (EELS, Ref. 21)										
Peak	Energies (eV)		Term value (eV)		Assignment, ^a this work (virtual orbital) C_{2v} or T_d					
1	155.07		2.83		unresolved b_1^*, b_2^*, a_1^*					
P^c	157.9		0							
2	173		-15.1		t_2^{*c}					
(c) Silicon 2p (EELS, Ref. 21 and photoionization yield, Ref. 22)										
Peak	Energy (eV)		Term value (eV)				Assignment, ^a this work C_{2v} or T_d			
	Ref. 21	Ref. 22	Ref. 21 $\frac{3}{2}$	Ref. 21 $\frac{1}{2}$	Ref. 22 $\frac{3}{2}$	Ref. 22 $\frac{1}{2}$	$\frac{3}{2}$	$\frac{1}{2}$		
1		103.0			2.94				} b_1^*, b_2^*, a_1^* } b_1^*, b_2^*, a_1^*	
1'	103.6	103.64		2.95		2.91				
2	104.19	104.18	1.75		1.76		1.94			
2'	104.73	104.61		1.82						
3		104.88			1.06					
3'	105.45	105.55		1.10		1.0				
$\frac{3}{2}P^c$	105.94		0							
$\frac{1}{2}P^c$	106.55			0						
4	105.97	107.0		0.58	-1.06				$e^{*c,d}$	
5	124.1		-17.86 ^e						t_2^{*c}	

^aThis assignment is made using the C_{2v} symmetry group for type-I resonance and T_d for type-II resonances.

^bSee text.

^cReference 21 and references therein.

^dReference 33.

^eUsing an average value for the $2p_{3/2}, 2p_{4/2}$ components.

under study. Available photoelectron spectra in the soft-x-ray range [x-ray photoemission spectroscopy (XPS)], have been considered. Only Si 2*p* spectra in TMS (Refs. 33–35), SiF₄ (Refs. 33 and 35–37), and SiCl₄ (Refs. 33 and 37) are known. They provide a direct measurement of 2*p* ionization energies with an accuracy ranging from 0.1 to 0.3 eV. For the Si 1*s* edge, no XPS value is available, except for SiH₄ (Ref. 38).

We have then determined the Si 1*s* ionization energy by two independent but indirect methods based on (i) an extrapolation of the Si 1*s* energy of SiH₄, and (ii) the Si 2*p* and *Kα* emission energies of silicon measured in related silicon compounds. The first method takes advantage of the excellent linear correlation of 1*s* shift (Δ_{1s}) with 2*p* shifts (Δ_{2p}) established by Sodhi and Cavell³⁹ on a large number of phosphorus and sulfur compounds. It is then

reasonable to assume a similar behavior for Si compounds using the relationship $\Delta_{1s} = 1.12\Delta_{2p}$ where 1.12 is a coefficient extrapolated from phosphorus compounds (1.14) and sulfur compounds (1.16). Knowing the 2*p* edge (107.1 eV) in SiH₄ from Kelfve *et al.*³⁷ we are then able to extract from the 1*s* edge energy in SiH₄ (1847.0±0.5 eV) and from the 2*p* edges of the three molecules under study the 1*s* energies of SiF₄ (1852.0±0.7 eV), TMS (1845.7±0.7 eV), and SiCl₄ (1850.5±0.7 eV).

The second method is based on the slight chemical shift (< 1 eV) of the Si *K-L*_{II,III} transition in a variety of silicon compounds⁴⁰ with respect to pure silicon.^{41,42} This transition is measured through the *Kα* emission line either in the molecule under study or in a closely related compound. We then add to this value the suitable Si 2*p* energy measured by XPS (Refs. 33, 35, and 37). For

TABLE III. Absolute energies (eV), term values (eV), and proposed assignment (virtual orbital) for resonances observed in the inner-shell spectra of SiCl₄.

(a) Silicon 1 <i>s</i> (photoabsorption, this work)					
Peak	Energy (eV)	Term value (eV)	Assignment ^a (C _{2v}) or (T _d)		
1	1843.8	6.8	unresolved b ₁ [*] , b ₂ [*] , a ₁ [*]		
2	1848.8	1.8	a ₁ [*]		
P ^b	1850.6	0			
3	1855.5	-4.9	t ₂ [*]		
4	1858.3	-7.7	t ₂ [*]		
5	1872.6	-22.0	t ₂ [*]		
(b) Silicon 2 <i>p</i> (photoabsorption, Ref. 23)					
Peak	Energy (eV)	Term value (eV)		Assignment, ^a this work (C _{2v}) or (T _d)	
		$\frac{3}{2}$	$\frac{1}{2}$	$\frac{3}{2}$	$\frac{1}{2}$
1	103.0	7.25			
1'	103.5			b ₁ [*] , b ₂ [*] , a ₁ [*]	
2	104.7	5.55			
2'	105.2			b ₁ [*] , b ₂ [*] , a ₁ [*]	
3	107.1	3.15			
4	108.5	1.75		a ₁ [*]	
4'	109			1.86	
$\frac{3}{2}P^c$	110.25				
$\frac{1}{2}P^c$	110.86				
5	115.8	-5.2 ^e			
6	122.8	-12.2 ^e		e ^{*d}	
7	134.5	-24 ^e		t ₂ ^{*d}	

^aThe suggested assignment is made for type-I resonances within the C_{2v} symmetry group and for type-II, within the T_d one.

^bSee text.

^cReference 33.

^dReferences 28 and 29.

^eUsing an average value for the 2*p*_{3/2}, 2*p*_{1/1} components.

SiCl₄, we have used the Si *Kα* line measured in SiO₂ by Costa-Lima⁴¹ at 1740.4 eV because SiO₂ is the closest compound to SiCl₄ as far as the electronegativity of the ligand is concerned. We then obtain a Si 1*s* core energy of 1850.6 eV. For TMS we have used the Si *Kα* emission measured in SiC by Senemaud³² at 1740.2 eV. The Si 1*s* energy is 1846.1 eV. For SiF₄ we have used the same emission line measured in Na₂SiF₆ by Faessler⁴³ at 1740.7 eV. We deduce the Si 1*s* energy value of 1852.3 eV. The overall accuracy of these Si 1*s* energies is estimated to be better than ±0.5 eV.

We observe that the Si 1*s* energies determined with these two methods are very similar. We have chosen the values obtained with the second method. Notice that for SiF₄ and SiCl₄ the Si 1*s* energies are very close to the value obtained indirectly by Szargan *et al.*⁴⁴

The Si 2*s* edge energy has been determined differently, because the *K-L*₁ radiative transition is forbidden and the corresponding emission line is not observed. The Si 2*s* and 2*p* energies are known in pure silicon to be at 151 and 99 eV (Ref. 45). Using the Si 2*p* shift in TMS or SiF₄ with respect to pure silicon, we have extracted the Si 2*s* edge energies in these two molecules, i.e. for TMS, 157.9 eV, and for SiF₄, 163.6 eV.

Knowing the absolute energies of resonances from our measured photoabsorption spectra, we readily extract the corresponding term values. They are reported for SiF₄, TMS, and SiCl₄ in Tables I, II, and III, respectively, together with term values extracted from the other available core spectra and reproduced in Figs. 1(b), 2(b), 2(c), 3(b), 3(c), and 3(d). These term values are used in the following discussion.

IV. DISCUSSION

The three molecules SiF₄ (Refs. 36 and 46), TMS (Ref. 35), and SiCl₄ (Ref. 47) have a tetrahedral geometry (*T_d* symmetry group) and a ¹*A*₁ ground state with the electronic configurations as seen in Table IV. Notice that in the three molecules, the Si 1*s* and Si 2*p* orbitals have the respective *a*₁ and *t*₂ symmetries. Consequently, because

*A*₁→*T*₂ is the only allowed dipole transition (see Table V), it is then likely that the most intense resonances in the Si 1*s* spectra will be due to excited states with *T*₂ symmetry. This means that, if a simple one-electron model can be used, type-I resonances result from the transition of a core electron into a *t*₂^{*} empty orbital and type-II resonances, i.e., shape resonances, belong to the *t*₂ partial channel.

In contrast, many transitions from the Si 2*p* core orbital can be expected because *T*₂→*A*₁, *E*, *T*₁, *T*₂ are all dipole allowed (see Table V). Notice that when the symmetry of the molecules decreases, more transitions are expected. This point is of particular importance for analyzing the specific case of type-I resonances.

A. Resonances in the discrete spectrum (type I)

Type-I resonances in SiX₄ (*X*=F, CH₃, or Cl) result from the promotion of a core electron (Si 1*s*, 2*s*, or 2*p*) into low-lying empty molecular orbitals. In the following we exclude, *a priori*, Rydberg orbitals because such transitions are known to carry low oscillator strength in nonhydride molecules.⁸ Such core excitation in SiX₄ compounds produces an additional electron in the valence-electron cloud. This observation justifies the comparison with the silicon equivalent core molecules PX₄ as suggested by Schwarz¹⁴ and Wittel and McGlynn.⁴⁸

PX₄ molecules are not stable species and are well-known phosphoranyl radicals in chemistry. Very interestingly, their most stable electronic configurations are found for geometries largely distorted from tetrahedral, namely a trigonal bipyramid (TBP). This fact is evidenced by single-crystal electron-spin-resonance experiments⁴⁹ and extensive theoretical analysis.^{50,51} Such PX₄ radicals can be thought of as pentavalent species with the odd electron acting as a sort of phantom ligand (Fig. 4). The ligands are separated into two distinct type of sites, axial and equatorial. Former studies found the most stable structure was TBP_e where the lone electron occupies an equatorial position, but recently Janssen *et al.*⁵¹ calculated the TBP_a geometry, where the lone electron is

TABLE IV. Electronic configurations for SiF₄, TMS, and SiCl₄.

Molecule	Core orbitals with parentage				Valence orbitals with parentage			
SiF ₄	1 <i>a</i> ₁ ² Si 1 <i>s</i>	1 <i>t</i> ₂ ⁶ 2 <i>a</i> ₁ ² F 1 <i>s</i>	3 <i>a</i> ₁ ² Si 2 <i>s</i>	2 <i>t</i> ₂ ⁶ Si 2 <i>p</i>	4 <i>a</i> ₁ ² 3 <i>t</i> ₂ ⁶ Si-F bond	5 <i>a</i> ₁ ² 4 <i>t</i> ₂ ⁶ 1 <i>e</i> ⁴ 5 <i>t</i> ₂ ⁶ 1 <i>t</i> ₁ ⁶ F lone pairs and Si-F bond		
Si(CH ₃) ₄	1 <i>a</i> ₁ ² Si 1 <i>s</i>	2 <i>a</i> ₁ ² 1 <i>t</i> ₂ ⁶ C 1 <i>s</i>	2 <i>a</i> ₁ ² Si 2 <i>s</i>	2 <i>t</i> ₂ ⁶ Si 2 <i>p</i>	4 <i>a</i> ₁ ² 3 <i>t</i> ₂ ⁶ Si-C bond	5 <i>a</i> ₁ ² 4 <i>t</i> ₂ ⁶ 1 <i>e</i> ⁴ 1 <i>t</i> ₁ ⁶ 5 <i>t</i> ₂ ⁶ C-H bond and Si-C bond		
SiCl ₄	1 <i>a</i> ₁ ² Si 1 <i>s</i>	1 <i>t</i> ₂ ⁶ 2 <i>a</i> ₁ ² Cl 1 <i>s</i>	3 <i>a</i> ₁ ² 2 <i>t</i> ₂ ⁶ Cl 2 <i>s</i>	4 <i>a</i> ₁ ² Si 2 <i>s</i>	5 <i>a</i> ₁ ² 3 <i>t</i> ₂ ⁶ 1 <i>e</i> ⁴ 1 <i>t</i> ₂ ⁶ 4 <i>t</i> ₁ ⁶ Cl 2 <i>p</i>	5 <i>t</i> ₂ ⁶ Si 2 <i>p</i>	6 <i>a</i> ₁ ² 6 <i>t</i> ₂ ⁶ Si-Cl bond	7 <i>a</i> ₁ ² 7 <i>t</i> ₂ ⁶ 2 <i>e</i> ⁴ 8 <i>t</i> ₂ ⁶ 2 <i>t</i> ₁ ⁶ Cl lone pairs and Si-Cl bond

TABLE V. Dipole-allowed transitions in the T_d , C_{3v} , C_{2v} symmetry groups.

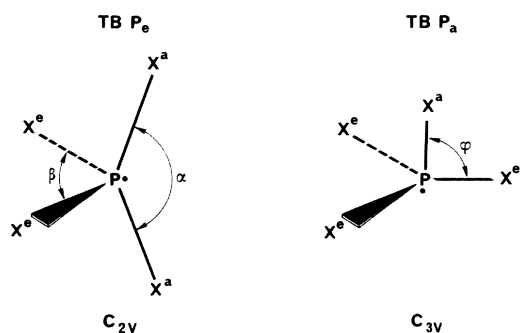
T_d	C_{3v}	C_{2v}
$a_1 \rightarrow t_2$	$a_1 \rightarrow a_1, e$	$a_1 \rightarrow a_1, b_1, b_2$
$a_2 \rightarrow t_1$	$a_2 \rightarrow a_2, e$	$a_2 \rightarrow a_2, b_1, b_2$
$e \rightarrow t_1, t_2$	$e \rightarrow a_1, a_2, e$	$b_1 \rightarrow a_1, a_2, b_1$
$t_1 \rightarrow a_2, e, t_1$		$b_2 \rightarrow a_1, a_2, b_2$
$t_2 \rightarrow a_1, e, t_1, t_2$		

in the axial position, to be the most stable. The vertical transition from a tetrahedron (T_d) (SiX_4 neutral molecule) to an excited state with equilibrium geometry of lower symmetry, leads to more electronically excited states than expected transitions within the T_d symmetry group (Table V). This removal of degeneracy of certain orbitals, as illustrated in Table VI, depends upon the symmetry group. These states are all vibrationally excited to conserve the total symmetry T_d . More importantly, such vibrations involve one (or more) distortion modes, normally forbidden by symmetry. Therefore one should invoke a vibronic coupling which departs from the Born-Oppenheimer approximation. This is also known as a Jahn-Teller effect (see, for example, Ref. 52) which is expected for all degenerate states (ground and excited). Such analysis has been performed successfully by Fernandez *et al.*⁵³ for another tetrahedral species SnH_4 . The SnH_4^+ ion is found to be more stable in the C_{2v} and C_{3v} symmetries and this explains the observed ionization transitions and removes the degeneracy of certain orbitals, as illustrated in Table VI.

Let us analyze now the ideal Si core-absorption spectra of SiX_4 molecules expected from the electronic structure of PX_4 radicals. Ground-state neutral PX_4 may be compared with the first excited state resulting from the transition of a Si core electron into a_1^* because, according to previous work, a_1^* is the lowest empty orbital of SiX_4 molecules¹ and the outermost singly occupied in PX_4 radicals.^{50,51} Notice that for degenerate core orbitals such as

TABLE VI. Relationships of species of the T_d symmetry group with C_{3v} and C_{2v} . The α , β , and φ angles are defined in Fig. 4 and refer to known geometries of PX_4 radicals.

C_{3v}	T_d	C_{2v}
$\varphi = 89^\circ - 99^\circ$	$\alpha = \beta = \varphi = 109.4^\circ$	$\alpha = 158^\circ - 172^\circ$ $\beta = 96^\circ$
a_1	a_1	a_1
a_2	a_2	a_2
a_1	t_2	a_1
e		b_1
a_2	t_1	a_2
e		b_1
e	e	a_1
		a_2

FIG. 4. Schematics of geometries of PX_4 radicals trigonal bipyramid "equatorial" or trigonal bipyramid "axial" within the respective C_{2v} or C_{3v} symmetry groups after Refs. 50 and 51.

Si $2p$, one expects to have two possible transitions because of spin-orbit coupling associated with the core vacancy, i.e., $\text{Si } 2p_{3/2} \rightarrow a_1^*$ and $\text{Si } 2p_{1/2} \rightarrow a_1^*$. The comparison of core excited Si X_4^* to PX_4 radicals is meaningful only if the lifetime of the considered species is large enough to produce a well-defined line in an absorption spectrum. In the present cases (this work and Refs. 1, 21, and 22) the observed linewidths are generally larger than the instrumental broadening and can be analyzed in terms of several contributions to the decay rates of the core excited states. The lifetime is firstly limited, for low- Z compounds, by electronic relaxation processes such as Auger, including Coster-Kronig decay.⁵⁴ The rate of Auger processes is expected to vary with the nature of the core hole.⁵⁴ For a $1s$ hole the most probable Auger process is KLL which gives the atom with two final vacancies in the $L_{II,III}$ core subshell ($2p$). Consequently, the overall rate of such an Auger process will be similar in all silicon compounds. An experimental value of 0.45 eV for the Si $1s$ linewidth has been evaluated by Senemaud³² in agreement with the value of 0.5 eV calculated by Keski-Rahkonen and Krause.⁵⁵ The decay of a $2s$ hole proceeds primarily through a Coster-Kronig transition, via the $2p$ shell. This process is generally faster than the normal Auger ones. Thus, Keski-Rahkonen and Krause⁵⁵ calculated a total decay rate of the Si $2s$ hole to be faster (~ 1.5 -eV linewidth) than that of the Si $1s$ hole. The same authors⁵³ found that the Si $2p$ hole decays by Auger decay at a much slower rate (~ 0.07 -eV linewidth). Indeed this has been confirmed by XPS experiments on crystalline silicon⁵⁶ which gives an upper limit of the $2p$ linewidth at 0.106 eV. In a molecule, the Auger decay of a $2p$ hole is likely to be slower than that in an atom. The presence of the two final holes in valence shells which are localized either on a Si- X bond or on ligand X , makes the Auger pro-

cess interatomic in character, and much less probable than intra-atomic Auger process.⁵⁷ Consequently, electronic relaxation processes are not sufficient to explain all of the observed widths.

Another cause of line broadening may be dissociation. This process essentially depends upon valence electrons and can be considered as totally independent of core electrons. In the present case, dissociation rates can be extracted from the stability of PX_4 radicals. We know from the recent theoretical analysis of Janssen *et al.*⁵¹ that the PX_4 ground state decays into $PX_3 + X$ with a possible transition state for PH_4 and PFH_3 but not for $PClH_3$. Unfortunately, no corresponding lifetime has been calculated. Nevertheless, if the extra broadening of some lines as observed in the $2p$ spectra of SiF_4 , for example, originates from dissociation, the associated rate lies on a femtosecond time scale. This exceptionally fast process should not be surprising because valence empty orbitals have a strong antibonding character and lead often to purely repulsive potential surfaces.⁵⁸ This is probably the case here.

We can also expect that the term value of the resonance (a_1^*) in the discrete part of the Si core-absorption spectra should be comparable to the first-ionization potential associated with the ejection of the outermost valence orbital of PX_4 radicals. Unfortunately, there are no experimental values available. However, for PF_4 , the theoretical value⁵⁹ of 9.93 eV compares favorably with the first-term value measured in the Si $1s$ spectrum of SiF_4 . This supports the assignment suggested below, of the lowest resonance [line 1 in Fig. 1(a)] to be associated with the a_1^* virtual orbital. We now analyze the real spectra presented in Figs. 1–3.

1. SiF_4

The first striking observation in the Si $1s$ spectrum is the presence in the discrete spectrum of a weak resonance followed by two intense structures separated by 1.4 eV. The lowest empty orbital in SiF_4 is known^{1,5,26} to have a_1 symmetry in the T_d symmetry group. We suggest then that the first line [line 1 in Fig. 1(a)] results from a transition into a_1^* . Its low intensity is due to the forbidden character of the transition (Table V). The interpretation of the intense doublet (lines 2 and 3) is more puzzling. The nondegenerate character of the Si $1s$ orbital (a_1 in T_d , C_{2v} , C_{3v}) and the probable weak spin-orbit coupling of the diffuse t_2^* (T_d) eliminates reasonably any significant splitting. Dipole selection rules in the T_d symmetry group imply that both intense structures have a t_2^* symmetry. This is in contradiction to various theoretical analyses^{1,5,26} performed in this geometry because only a a_1^* empty orbital followed by a single t_2^* one are expected. Consequently, we have analyzed the spectrum using the comparison with the core equivalent radical PF_4 . If we assume that the Si core-excited states do not have a tetrahedral geometry but rather a C_{2v} or C_{3v} one, we expect though a Jahn-Teller effect (see Table VI) a single transition $a_1 \rightarrow a_1^*$, and two transitions (C_{3v}) $a_1 \rightarrow a_1^*$, e^* or three transitions (C_{2v}) $a_1 \rightarrow a_1^*$, b_1^* , b_2^* depending on the equilibrium final-state geometry. We offer then the possible assignments as indicated in Table I. The intense doublet which has a very pronounced asymmetry on its

high-energy side is then easily interpreted as a transition in the C_{3v} geometry (a_1^* , e^*) or may be in the C_{2v} one (a_1^* , b_1^* , b_2^*). In the latter case, either two of the three transitions are energy degenerate or the third member has a very small intensity. Notice that such a transition is surely accompanied by a large amount of vibrational excitation for conservation of the total symmetry (see above) and it is impossible without suitable calculations to give a reasonable ordering of virtual orbitals. Nevertheless, we suggest (not indicated in Table I) that the lowest peak of the intense doublet is associated with the antibonding Si-F axial orbital and the highest peak to the Si-F equatorial one. This is based on the longer Si-F bond for axial than for equatorial fluorine atoms, in the TBP_e geometry.⁵¹ A reverse suggestion must be made in the TBP_a geometry, for which the Si-F axial bond is shorter than the Si-F equatorial one.⁵¹

In contrast to the Si $1s$ spectrum, the Si $2s$ one obtained by Friedrich *et al.*¹ reveals a single broad maximum. We believe that this structure “hides” the doublet because of the $2s$ lifetime hole which is probably much shorter. Notice that if there is a 1.4-eV separation between resonances, a Coster-Kronig transition (1.5-eV linewidth) for each line is sufficient to explain the observed broadening of ~ 3 eV.

The Si $2p$ spectrum as obtained by Friedrich *et al.*¹ is much richer. In this case, the Si $2p$ hole lifetime is long (see above) and all expected features are doubled because of spin-orbit splitting of the $2p$ hole. Former assignments^{1,5,9,25} all agree to assign line 1,1' as transition to a_1^* (T_d), the lowest virtual orbital of SiF_4 . The change in geometry (C_{2v} or C_{3v}) does not change this assignment (see Table VI). However, if we assume the second virtual orbital to be t_2^* , following Pavlychev *et al.*⁹ we again expect three components in the C_{2v} geometry or two in the C_{3v} geometry. Consequently, we expect six peaks (C_{2v}) and four peaks (C_{3v}) because of spin-orbit splitting. Indeed the Si $2p$ spectrum shows six peaks which seems to confirm an analysis within a C_{2v} geometry. We believe that this interpretation is more attractive than the previous interpretation of Friedrich *et al.*,¹ Robin,⁵ or Hayes and Brown²⁶ who interpreted this series of six peaks as a transition to t_2^* with some others to various Rydberg orbitals. Indeed Friedrich *et al.*¹ have founded their interpretation on the comparison with the solid SiF_4 spectrum. We think that their observation is not incompatible with the present interpretation considering that in the condensed phase, a C_{3v} geometry may be found with only two empty orbitals, a_1^* and e^* (Table VI).

Our interpretation of the three core photoabsorption spectra of SiF_4 implies that there is no transferability of term values. This is probably due to significant variation of J and K integrals but this point should be clarified with theoretical calculations.

2. $Si(CH_3)_4$

The large and asymmetric peak of the Si $1s$ and Si $2s$ spectra of TMS may also be interpreted using a Jahn-Teller effect on the basis of the Si core equivalent radical $P(CH_3)_4$. It is possible that the combination of a small distortion and short lifetime of each “component” of a

split t_2 empty orbital explains the Si 1s peak shape. This interpretation is supported by the fine structures of the Si 2p spectrum obtained by Sodhi *et al.*²¹ and Morin²² [see Figs. 2(b) and 2(c) and Table II]. Indeed, there are six features [Fig. 2(c)] in the discrete part of the spectrum which are distinct from another resonance right above threshold.^{34,60} These small features are similar to those of the Si 2p spectrum of SiF₄ just below the edge. Consequently, we suggest that the core excited state has a C_{2v} geometry which splits the transition to $t_2^*(T_d)$ into a_1^* , b_1^* , b_2^* components. The spin-orbit splitting of the Si 2p hole would explain the observation of six features. This interpretation contrasts somewhat with those of Sodhi *et al.*²¹ who suggest a transition to a $\sigma^*(a_1, t_2)$ orbital with an admixture of Rydberg transitions. But very interestingly, Sodhi *et al.*²¹ noticed the missing 4s Rydberg transition combined with the impossibility of fitting these structures with regular Rydberg formula or with a vibrational progression. We believe that indeed there is a contribution of the σ^* transition following Sodhi *et al.*²¹ but it is a strictly t_2^* one (without any Rydberg contribution) and is split by the removal of degeneracy, expected in a Jahn-Teller effect as discussed above, and the spin-orbit coupling.

Notice that there is no observable transition to a_1^* . This is not so surprising if the tetrahedron is only slightly distorted and does not bring much intensity to the "forbidden" transition to a_1^* . Like for SiF₄, in this interpretation there is poor transferability of term values.

3. SiCl₄

The observation of two well-separated features in the discrete part of the spectrum contrasts drastically with the SiF₄ and TMS cases. The analysis of the Si 2p spectrum obtained by Zimkina and Vinogradov²³ shows that the envelope of peaks 1 and 2 (lines 1', 2') in Fig. 3(b) matches peak 1 in Fig. 3(a) (see also Table III). In addition, peak 2 in Fig. 3(a) seems to correspond to feature 4 in Fig. 3(b). The use of the Si core equivalent PCl₄ radical which is known⁴⁹ to have a distorted geometry (C_{2v}) (see Fig. 4) does not help readily to interpret the spectrum. We suggest then that the lowest set of peaks in the Si 2p spectrum does result from a splitting of the transition to a t_2^* orbital (T_d). But the distortion would be much smaller than in the preceding cases, the "geometrical" splitting would be small compared to the 1s linewidth but slightly larger than the 2p one. The interpretation of the second peak in the Si 1s spectrum which seems to be split (lines 4, 4') by spin orbit in the Si 2p spectrum is more puzzling. Firstly, its low intensity may be explained using a a_1^* assignment, having in mind that the Si 1s $\rightarrow a_1^*$ transition is forbidden in the T_d symmetry group, but no a_1^* virtual orbital has been calculated above the t_2^* one. Secondly, the presence of Rydberg levels, which may be supported by the additional feature such as line 3 in the Si 2p spectrum, is not very convincing; the large size of the chlorine ligands are likely to "mask" any significant contribution of "outerwell" states such as Rydberg states. We then offer the assignment of Table III, which supposes a reversal of the t_2^* and a_1^* virtual orbitals compared to SiF₄.

Notice that unlike SiF₄ and TMS, the transferability of term values is rather satisfactory.

B. Resonances in the continuum (type II)

Such resonances are often due to the shape (potential barrier) of the molecular potential seen by the outgoing electron. Notice, as mentioned in the Introduction, that type-I resonances may also result from the shape of the potential, however, the distinction between both types holds because, for type-I resonances, the ejection of the core electron is energetically impossible, in contrast to type-II resonances. Consequently, type-I resonances decay through various types of multiexcitation and multiionization processes (autoionization, Auger, Coster-Kronig, etc.) (Ref. 6) which are often slower than one-electron processes such as direct ionization or shape resonances. It generally results that type-II resonances are much broader than type-I resonances. An immediate consequence is that the outgoing electron does not stay long enough for the valence electron cloud to "destroy" the original tetrahedral geometry of the neutral molecule. In a core-equivalent model, the electron interacts with a SiX_4^+ (with a core hole) which is equivalent to the ground-state PX_4^+ ion. Indeed, it has been predicted⁵⁰ that this ion is probably tetrahedral. Consequently, there is no need to invoke Jahn-Teller effects to analyze the continuum features. The partial channels of the photoionization cross section associated with the nl subshells are governed by dipole-transition selection rules, i.e., the energy dependence of the matrix elements of the $a_1 \rightarrow t_2$ and $t_2 \rightarrow a_1, e, t_1, t_2$ transitions. It is clear that then shape resonances observed in the Si 1s continuum in tetrahedral molecules are mainly expected in the t_2 partial channel. This is indeed what is predicted by Carlson *et al.*²⁹ in SiCl₄ using multiple-scattering theory. They calculate for the Si 2s continuum two resonances at 10 and 20 eV above the edge in the t_2 partial channel. There are no experimental results available for SiCl₄ near the Si 2s edge but we may analyze the present Si 1s photoabsorption of SiCl₄ along the same lines since we are dealing with a core orbital with the same symmetry. We indeed find two broad features at 7.7- and 22.0-eV electron energy which are likely shape resonances in the t_2 continuum. We have found, moreover, and additional resonance at 4.6-eV electron energy which has not been calculated yet. Notice that the recent experimental work on the Si 2p partial cross section in SiCl₄ by Carlson *et al.*²⁹ reveals two distinct resonances at 15- and 24-eV electron energy. Pavlychev *et al.*²⁷ has observed in the Si 2p photoabsorption spectrum three features located at 5.6, 15, and 26 eV. The theoretical analysis (multiple-scattering $X\alpha$ model) of Carlson *et al.*²⁹ and Pavlychev *et al.*²⁷ are in reasonable accord in assigning the 15-eV one with a e^* symmetry and the 24-eV one with a t_2^* symmetry. The feature at 5.6 eV (Ref. 27) has not been interpreted. It probably corresponds with the additional 4.6-eV feature seen in our spectrum.

For TMS there are no calculations available. However, we suggest that the broad and intense resonance line 2 in Fig. 2(a) is likely a t_2 -shape resonance. A similar sugges-

tion has been offered by Sodhi *et al.*²¹ for line 2 in the Si 2s electron-energy-loss spectrum of Fig. 2(b). In the Si 2p photoabsorption we note that the upper part of the broad resonance across the edge and the broad line (line 5), beyond the edge, have been respectively assigned to shape resonances with e^* and t_2^* symmetry by Sodhi *et al.*²¹ and de Souza *et al.*³⁴

In the Si 1s continuum of SiF₄ one can similarly assign the broad features 4 and 5 to the t_2 partial channel. Unlike TMS the available 2s photoabsorption spectrum of SiF₄ (Ref. 1) is in a too-narrow range to be compared with the Si 1s results. In contrast, Pavlychev *et al.*^{9,28} have made detailed calculations using the multiple-scattering X_α theoretical model of resonances in the Si 2p continuum. They found that the first resonance (line 5) dominates the e^* continuum while the second (line 6) is probably present in both the e and t_2 continua.

V. CONCLUSIONS

Resonances observed in the present Si 1s photoabsorption spectra of SiF₄, Si(CH₃)₄, and SiCl₄ are qualitatively interpreted using a comparison to the Si core equivalent species which are the phosphoranyl radicals PX_4 ($X = F, CH_3,$ and Cl). The distortion of tetrahedron geometry into the trigonal bipyramid geometry of such radicals, accompanied by vibrational excitation, through a Jahn-Teller interaction explains the removal of the degeneracy of the transitions into t_2^* empty orbitals as defined in a T_d symmetry group. This distortion is probably large for SiF₄ but less pronounced for TMS and SiCl₄. It is possible that similar effects probably exist in CX_4 compounds, with NX_4 core equivalent species, but the C 1s EELS spectra^{61,62} must be reinterpreted. Such interpretation

may be of high interest in searching for "stable" isomers or excited states of PX_4 radicals in which the unpaired electron lies in one of the t_2 molecular orbitals defined in the tetrahedral geometry. The nontransferability of term values (except for SiCl₄) raises the question of the core-energy dependence of Coulomb and exchange integrals.

Resonances observed in the Si 1s continuum of the three molecules are likely t_2^* shape resonances because of dipole selection rules. The use of a pure tetrahedral geometry is justified by the extremely short stay of the outgoing electron in the valence region of the molecule. Multiple-scattering calculations are strongly needed to confirm the one-electron character of the observed resonances and find out by difference any evidence for doubly excited states. Lastly, the present observation and identification of intense resonances near the SiK edge in silicon compounds may shed some light on the recent observation of a giant resonance near the SiK edge in pure silicon and solid SiO₂ observed by Costa-Lima⁴¹ and by Hecht *et al.*⁶³

ACKNOWLEDGMENTS

We are grateful to R. N. Sodhi for very helpful suggestions about Si 1s core energy-level determination and A. P. Hitchcock for a critical reading of the manuscript. We warmly thank C. Senemaud for providing us with her results prior to publication. We are indebted to the LURE staff for the general facilities and for operating the ACO storage ring. LURE is a Laboratoire Commun Centre National de la Recherche Scientifique, Commissariat à l'Energie Atomique, et Ministère de l'Education Nationale.

- ¹H. Friedrich, B. Pittel, P. Rabe, W. H. E. Schwarz, and B. Sonntag, *J. Phys. B* **13**, 25 (1980).
- ²J. Nordgren and C. Nordling, *Comments Atom. Mol. Phys.* **13**, 229 (1983); J. H. Fock and E. E. Koch, *Chem. Phys.* **96**, 125 (1985).
- ³J. L. Dehmer, *J. Chem. Phys.* **56**, 4496 (1972).
- ⁴W. H. E. Schwarz, *Chem. Phys.* **9**, 157 (1975); **11**, 217 (1975).
- ⁵M. B. Robin, *Chem. Phys. Lett.* **31**, 140 (1975).
- ⁶G. Wendin, in *EXAFS and Near Edge Structure*, Vol. 27 of *Springer Series in Chemical Physics*, edited by A. Bianconi, L. Incoccia, and S. Stipcich (Springer-Verlag, Berlin, 1983), p. 29.
- ⁷R. D. Deslattes, R. E. LaVilla, P. L. Cowan, and A. Henins, *Phys. Rev. A* **27**, 923 (1983).
- ⁸R. N. S. Sodhi and C. E. Brion, *J. Electron Spectrosc. Relat. Phenom.* **34**, 373 (1984); **36**, 187 (1985); R. N. S. Sodhi, C. E. Brion, and R. G. Cavell, *J. Electron Spectrosc. Relat. Phenom.* **34**, 373 (1984).
- ⁹A. A. Pavlychev, A. S. Vinogradov, T. M. Zimkina, D. E. Onopko, and S. A. Titov, *Opt. Spektrosk.* **52**, 506 (1982) [*Opt. Spectrosc. (USSR)* **52**, 302 (1982)].
- ¹⁰S. Bodeur and J. M. Esteve, *Chem. Phys.* **100**, 415 (1985).
- ¹¹T. M. Zimkina and A. S. Vinogradov, *Izv. Akad. Nauk USSR Ser. Fiz.* **36**, 248 (1972) [*Bull. Acad. Sci. USSR, Phys. Ser.* **36**,

229 (1972)].

- ¹²R. E. LaVilla, *J. Chem. Phys.* **57**, 899 (1972).
- ¹³A. P. Hitchcock, C. E. Brion, *Chem. Phys.* **33**, 55 (1978).
- ¹⁴W. H. E. Schwarz, *Chem. Phys.* **11**, 217 (1975).
- ¹⁵N. Kosugi and H. Kurada, *Chem. Phys. Lett.* **94**, 377 (1983).
- ¹⁶G. R. Wight and C. E. Brion, *J. Electron Spectrosc. Relat. Phenom.* **4**, 325 (1974); G. R. Wight, C. E. Brion, and M. J. Van Der Wiel, *J. Electron Spectrosc. Relat. Phenom.* **1**, 457 (1972/1973).
- ¹⁷D. A. Shaw, G. C. King and F. H. Read, *J. Phys. B* **13**, L723 (1980).
- ¹⁸G. R. Wight and C. E. Brion, *J. Electron Spectrosc. Relat. Phenom.* **3**, 191 (1974).
- ¹⁹A. P. Hitchcock and C. E. Brion, *Chem. Phys.* **37**, 319 (1979).
- ²⁰D. L. Mott, *Phys. Rev.* **144**, 94 (1966).
- ²¹R. N. S. Sodhi, S. Daviel, C. E. Brion, and G. G. B. De Souza, *J. Electron Spectrosc. Relat. Phenom.* **35**, 45 (1985).
- ²²P. Morin, *Photophysics and Photochemistry above 6 eV*, edited by F. Lahmani (Elsevier, Amsterdam, 1985), p. 1; P. Morin, P. Lablanquie, G. G. De Souza, and I. Nenner (unpublished).
- ²³T. M. Zimkina and A. S. Vinogradov, *J. Phys. (Paris) Colloq.* **32**, C4-3 (1971).
- ²⁴V. A. Fomichev, T. M. Zimkina, A. S. Vinogradov, and A. M. Evdokimov, *Zh. Strukt. Khim.* **11**, 676 (1970).

- ²⁵A. S. Vinogradov and T. M. Zimkina, *Opt. Spektrosk.* **31**, 288 (1971).
- ²⁶W. Hayes and F. C. Brown, *Phys. Rev. A* **6**, 21 (1972).
- ²⁷A. A. Pavlychev, A. S. Vinogradov, T. M. Zimkina, D. E. Onopko, and S. A. Titov, *Opt. Spektrosk.* **47**, 7378 (1979) [*Opt. Spectrosc. (USSR)* **47**, 40 (1979)].
- ²⁸A. A. Pavlychev, A. S. Vinogradov, and T. M. Zimkina, *Opt. Spektrosk.* **52**, 231 (1982) [*Opt. Spectrosc. (USSR)* **52**, 139 (1982)].
- ²⁹T. A. Carlson, W. A. Svensson, M. O. Krause, T. A. Whitley, F. A. Grimm, G. Von Wald, J. W. Taylor, B. P. Pullen, *J. Chem. Phys.* **84**, 122 (1986).
- ³⁰M. Lemmonier, O. Collet, C. Depautex, J. M. Esteva, and D. Raoux, *Nucl. Instrum. Methods* **152**, 109 (1978).
- ³¹D. M. Barrus, R. L. Blake, A. J. Burek, K. C. Chambers, and A. L. Pregenzer, *Phys. Rev. A* **20**, 104 (1979).
- ³²C. Senemaud, (private communication).
- ³³W. B. Perry and W. L. Jolly, *Inorg. Chem.* **13**, 1211 (1974).
- ³⁴G. G. B. De Souza, P. Morin, and I. Nenner, *J. Chem. Phys.* **83**, 492 (1985).
- ³⁵S. Aksela, K. H. Tan, H. Aksela, and G. M. Bancroft, *Phys. Rev. A* **33**, 258 (1986).
- ³⁶W. B. Perry and W. L. Jolly, *J. Electron Spectrosc.* **4**, 219 (1974).
- ³⁷P. Kelfve, P. Blomster, H. Siegbahn, and K. Siegbahn, *Phys. Scr.* **21**, 75 (1980).
- ³⁸R. G. Cavell and R. N. S. Sodhi, *J. Electron Spectrosc. Relat. Phenom.* **15**, 145 (1979).
- ³⁹R. N. Sodhi and R. G. Cavell, *J. Electron Spectrosc. Relat. Phenom.* **32**, 283 (1983); (to be published).
- ⁴⁰V. I. Sokolenko, E. A. Zhurakovskii, and A. I. Sokokenko, *Phys. Metals* **3**, 834 (1981).
- ⁴¹M. T. Costa-Lima, Thèse de doctorat d'état, Université de Paris VI, 1976.
- ⁴²Y. Cauchois and C. Senemaud, *Wavelengths of X-ray Emission Lines and Absorption Edges* (Pergamon, New York, 1978).
- ⁴³A. Faessler, in *Proceedings of the Tenth Colloquium Spectroscopicum International*, edited by E. R. Lippincott and M. E. Margoshes (Starpen, Washington, 1963)
- ⁴⁴R. Szargan, A. Meisel, E. Hartmann, and G. Brunner, *Jpn. J. Appl. Phys.* **17**, Supp. 17-2, 174 (1979).
- ⁴⁵C. Gahwiller, and F. C. Brown, *Phys. Rev. C* **2**, 1918 (1970).
- ⁴⁶G. Bicri, L. Asbrink, and W. Von Niessen, *J. Electron Spectrosc. Relat. Phenom.* **27** 129 (1982).
- ⁴⁷T. A. Carlson, A. Fahlman, M. O. Krause, T. A. Whitley, F. A. Grimm, M. N. Piancastelli, and J. W. Taylor, *J. Chem. Phys.* **84**, 641 (1986).
- ⁴⁸K. Wittel and S. P. Mc Glynn, *Chem. Rev.* **77**, 745 (1977).
- ⁴⁹A. Hasegawa, K. Ohnishi, K. Sogabe, M. Miura, *Mol. Phys.* **30**, 1367 (1975). J. H. H. Hamerlinck, P. Schipper, and H. M. Buck, *J. Am. Chem. Soc.* **105**, 385 (1983).
- ⁵⁰J. M. Howell and J. L. Olsen, *J. Am. Chem. Soc.* **98**, 7119 (1976).
- ⁵¹R. A. J. Janssen, G. J. Visser, and H. M. Buck, *J. Am. Chem. Soc.* **106**, 3429 (1984).
- ⁵²J. H. D. Eland, *Photoelectron Spectroscopy* (Butterworths, London, 1984).
- ⁵³J. Fernandez, J. Arriau, and A. Dargelos, *Chem. Phys.* **94**, 397 (1985).
- ⁵⁴J. Nordgren and H. Agren, *Comments At. Mol. Phys.* **14**, 203 (1983).
- ⁵⁵O. Keski-Rahkonen and M. O. Krause, *At. Data Nucl. Data Tables* **14**, 139 (1974).
- ⁵⁶L. Ley, J. Reichardt, and R. L. Johnson, *Phys. Rev. Lett.* **49**, 1664 (1982).
- ⁵⁷T. D. Thomas and P. Weightmann, *Chem. Phys. Lett.* **81**, 325 (1981).
- ⁵⁸P. Morin and I. Nenner, *Phys. Rev. Lett.* **56**, 1913 (1986).
- ⁵⁹J. Weber and M. Geoffroy, *Theor. Chim. Acta* **43**, 299 (1977).
- ⁶⁰P. Morin, G. G. B. De Souza, I. Nenner, and P. Lablanquie, *Phys. Rev. Lett.* **56**, 131 (1986).
- ⁶¹G. R. Wight and C. E. Brion, *J. Electron Spectrosc. Relat. Phenom.* **4**, 327 (1974).
- ⁶²A. P. Hitchcock and C. E. Brion, *J. Electron Spectrosc. Relat. Phenom.* **14**, 417 (1978).
- ⁶³M. H. Hecht, F. J. Gruenthaner, P. Pianetta, H. Y. Cho, M. L. Shek, and P. Mahowald, *EXAFS and Near Edge Structure*, edited by K. O. Hodgson, B. Hedman, and J. E. Pennet-Hahn (Springer-Verlag, Berlin, 1984), Vol. III, p. 67.